Ab Initio Study of Energetics of Protonation and Hydrogen Bonding of Pyridine *N*-Oxide and Its Derivatives

Mariusz Makowski, Adam Liwo,* Roman Wróbel, and Lech Chmurzyński

Faculty of Chemistry, University of Gdańsk, Sobieskiego 18, 80-952 Gdańsk, Poland

Received: July 1, 1999

The energetics of protonation and hydrogen-bonded complex formation between the base and its conjugated acid (homoconjugation) of pyridine *N*-oxide and its selected derivatives was investigated by means of Restricted Hartree-Fock (RHF) and Møller-Plesset (MP2) ab initio calculations. It has been found that introducing the *d* polarization functions (the 6-31G* basis set) is required to reproduce correctly the geometry of the N−O bond. The proton-transfer energy surface in the homoconjugated cations exhibits a double minimum, with 2.4 kcal/mol energy barrier for the pyridine *N*-oxide homocomplex; this barrier vanishes when the thermodynamic correction is included. The protonation and homoconjugation Gibbs free energies computed in vacuo correlate well with the acid dissociation and cationic homoconjugation constants determined in acetonitrile.

Introduction

Acid−base equilibria involving pyridine *N*-oxide derivatives (see Figure 1 for structure) are complicated because of a strong tendency of these compounds to form hydrogen-bonded complexes with their conjugated acids (the so-called homocomplexes). Therefore, the dominant equilibria set up in systems containing *N*-oxides and their conjugated acids can be written as eqs 1 and 2, respectively (with B denoting the *N*-oxide molecule).

$$B + H^+ \rightleftharpoons BH^+ \quad (1)$$

$$BH^+ + B \rightleftharpoons BHB^+ \quad (2)$$

The corresponding equilibrium constants K_a (acid dissociation constant) and K_h (cationic homoconjugation constant) are defined by eqs 3 and 4, respectively.

$$K_a = \frac{[H^+][B]}{[BH^+]} \quad (3)$$

$$K_h = \frac{[BHB^+]}{[B][BH^+]} \quad (4)$$

Homoconjugation equilibria have been proven to exist in many aprotic Parker solvents (e.g., acetonitrile or propylene carbonate).[1−4] The hydrogen bond in the homocomplex is exceptionally short, as revealed by X-ray crystallography,[5−9] which results in its high strength, leading to the presence of a considerable amount of homoconjugated cations even in polar solvents.[1] Several papers have been published[10−14] that refer to the determination of the acidity and homoconjugation constants of protonated *N*-oxides in various solvents, with the use of potentiometric and UV-spectroscopic methods. Given the considerable amount of experimental data, we thought it worthwhile to undertake a comparative theoretical study of protonation and hydrogen-bonding phenomena of this interesting class of compounds. We have chosen pyridine *N*-oxide (PyO) and its 2-methyl (2-PicO), 3-methyl (3-PicO), 4-methyl (4-PicO), 4-nitro ($4NO_2PyO$), 4-methoxy (4-MeOPyO), and 4-N′,N′-dimethyl ($4NMe_2PyO$) derivatives, which exhibit a broad range of acid−base and hydrogen-bonding properties.[1] Theoretical studies of the prototropic phenomena of pyridine *N*-oxide and its derivatives reported so far include only early semiempirical Complete Neglect of Differential Overlap (CNDO/2) and Modified Neglect of Diatomic Overlap (MNDO) studies of protonation[15] and homocomplex formation,[16] a 4-31G Restricted Hartree-Fock (RHF) ab initio study of protonation and homoconjugation of PyO and some of its 4-substituted derivatives,[17] and a recent 6-31G* RHF ab initio study of homocomplex formation of the unsubstituted pyridine *N*-oxide.[9]

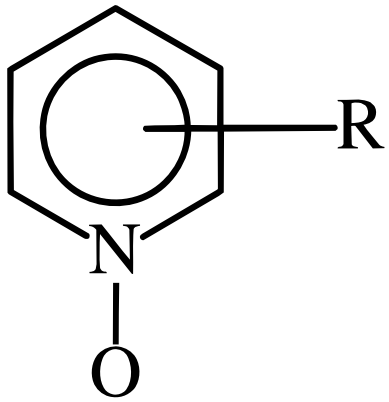

Figure 1. Molecular structure of pyridine *N*-oxide derivatives.

Methods

Closed-shell RHF ab initio calculations were carried out on pyridine *N*-oxide derivatives, their conjugated acids, and homoconjugated cations, using the program GAMESS.[18] The 6-31G* basis set was used for all compounds; for the PyO species additional calculations were also performed with the

* Corresponding author. Phone: +48 58 345 0361; fax: +48 58 341 0357; e-mail: adam@rutyl.chem.univ.gda.pl.

10.1021/jp9922662 CCC: $18.00
Published on Web 11/18/1999

TABLE 1: Selected Geometric Parameters of Pyridine *N*-Oxide Derivatives, Their Cationic Acids, and Homoconjugated Complexes

	PyO					2PicO		3PicO		4PicO		$4NO_2PyO$		4MeOPyO	$4NMe_2PyO$	
	6-31G	6-31+G	6-31G*	6-31+G*	exp.[a]	6-31G*	exp.[b]	6-31G*	exp.[c]	6-31G*	exp.[d]	6-31G*	exp.[d]	6-31G*	6-31G*	exp.[e]
Neutral Compound																
N-O	1.36	1.37	1.28	1.28	1.29	1.28		1.27		1.28	1.41	1.25	1.30	1.29	1.30	1.34
C-N	1.34	1.34	1.34	1.34	1.38	1.35		1.34		1.34	1.43	1.35	1.37	1.33	1.33	1.34
C-N-C	121.1	121.3	120.3	119.5	120.9	120.5		119.7		119.0	125.6	119.8	120.2	118.9	118.2	119.1
Cationic Acid																
N-O	1.39	1.39	1.35	1.35	1.38	1.36		1.36		1.35		1.35		1.36	1.36	
C-N	1.34	1.34	1.335	1.34	1.30	1.34		1.34		1.34		1.33		1.33	1.34	
C-N-C	124.0	124.0	123.8	123.8	126.1	124.7		124.0		123.0		124.1		122.5	121.6	
Homoconjugated Cation																
Na-Oa[f]	1.38	1.38	1.32	1.35	1.36	1.32	1.34	1.32	1.36	1.32	1.34	1.31		1.33	1.33	
Nb-Ob	1.37	1.37	1.35	1.32	1.36	1.35	1.34	1.35	1.36	1.35	1.34	1.34		1.35	1.35	
Ca-Na	1.34	1.34	1.33	1.33	1.34	1.34	1.41	1.33	1.33	1.33	1.32	1.33		1.32	1.33	
Cb-Nb	1.33	1.33	1.33	1.33	1.34	1.34	1.41	1.33	1.33	1.33	1.32	1.33		1.33	1.33	
Oa···Ob	2.45	2.45	2.54	2.56	2.41	2.53	2.39	2.52	2.41	2.51	2.44	2.54		2.52	2.51	
Ca-Na-Ca	123.4	123.5	121.1	123.3	122.6	121.8	123.7	121.3	124.2	120.5	120.0	121.3		120.2	119.4	
Cb-Nb-Cb	122.3	122.1	123.2	121.2	122.6	124.0	123.7	123.3	124.2	122.4	120.0	123.6		122.1	121.1	

[a] Ref 35 for neutral compound, 36 for cationic acid, and 8 for homoconjugated cation. [b] Ref 6 for neutral compound and 7 for homoconjugated cation. [c] Ref 8 for homoconjugated cation. [d] Ref 35 for neutral compound and 8 for homoconjugated cation. [e] Ref 37 for neutral compound. [f] a and b label the proton-donor and proton acceptor molecule, respectively.

6-31G, 6-31+G, and 6-31+G* basis sets. All species were subjected to unconstrained geometry optimization. After optimization was completed for a given species, the energy Hessian matrix was calculated to check whether the stationary point found was a true minimum and to compute the harmonic entropy and zero-point energy (see eqs 7 and 8).

Because the parallel code for the analytical Møller-Plesset (MP2) energy gradient was not available, it was infeasible to carry out geometry optimization with the inclusion of the dynamic correlation at the MP2 level (e.g., a single energy evaluation for the $PyOH^+\cdots PyO$ homoconjugated cation takes more than 5 h with one processor of the SUN E10K or the CRAY T3E supercomputer). Therefore, to estimate the effect of dynamic correlation we carried out just single-point MP2 calculations for the RHF-optimized structures.

The evaluation of the solvation contributions to the protonation and homoconjugation energies was attempted by using the self-consistent reaction field (SCRF) model, in which the solvent is represented as a continuous dielectric and the solute as a spherical cavity of a given radius immersed in this dielectric.[19−22] The radius of the cavity was calculated as the maximum dimension of the species studied plus 1 Å, according to the procedure described in the literature.[21] The dielectric constant was assigned the value of $D = 35.94$ for acetonitrile.[23] These calculations were carried out for fixed geometries corresponding to structures optimized in vacuo.

The protonation and homoconjugation energies are defined by eqs 5 and 6, respectively:

$$\Delta E_{prot} = E_{BH^+} - E_B \tag{5}$$

$$\Delta E_h = E_{BHB^+} - (E_B + E_{BH^+}) \tag{6}$$

The Gibbs free energies of protonation and homoconjugation were calculated from eqs 7 and 8, respectively.

$$\Delta G_{prot} = \Delta E_{prot} + \Delta E^\circ_{vib;prot} + p\Delta V_{prot} - T\left[(S_{vib;BH^+} + S_{rot;BH^+}) - (S_{vib;B} + S_{rot;B}) - \frac{3}{2}R\right] \tag{7}$$

$$\Delta G_h = \Delta E_h + \Delta E^\circ_{vib;h} + p\Delta V_h - T\left[(S_{vib;BHB^+} + S_{rot;BHB^+}) - (S_{vib;BH^+} + S_{rot;BH^+} + S_{vib;B} + S_{rot;B}) - \frac{3}{2}R\right] \tag{8}$$

where $\Delta E^\circ_{vib;prot}$ and $\Delta E^\circ_{vib;h}$ are the differences between the zero-point vibrational energies of the products and those of the substrates, respectively (these quantities can be calculated from eqs 5 and 6 after substituting $E^\circ_{X;vib}$ for E_X), p is the pressure, V is the volume of a system; in both cases assuming the ideal gas equation-of-state, we have $p\Delta V = RT\Delta n = -RT$, because $\Delta n = -1$ (n being the number of moles); S_{rot} and S_{vib} are the rotational and vibrational entropies, respectively (S_{vib} is calculated in the harmonic approximation) and the contribution $3/2R$ in eqs 7 and 8 arises from the fact that the system is composed of two chemical individuals before protonation or homoconjugation takes place, and of one after the corresponding reaction has occurred; this implies losing three translational degrees of freedom. A temperature of 298 K and pressure of 1 atm were assumed in all calculations. It should be noted that eqs 7 and 8 describe the energetics of protonation and homoconjugation in vacuo.

The proton-transfer curve in the $PyOH^+\cdots PyO$ homocomplex was calculated by carrying out a series of constrained energy minimizations with the O−H distance fixed at a given value and optimizing the remaining degrees of freedom.

Results and Discussion

Selected calculated geometric parameters of pyridine *N*-oxide and its derivatives, their conjugated acids, and homoconjugated cations, as well as the available experimental data are summarized in Table 1. The bond lengths and angles calculated with the 6-31G* basis set are in reasonable agreement with the available experimental data, whereas without the polarization functions the calculated lengths of the N− O bonds are about 0.08 Å longer than the corresponding experimental values. In the case of 4 PicO, the experimental N−O bond length is longer than the one calculated with the 6-31G* basis set; however, the experimental value seems to be excessive, in comparison with the data of other PyO derivatives. The inclusion of diffuse functions on heavy atoms (extension of the basis set to

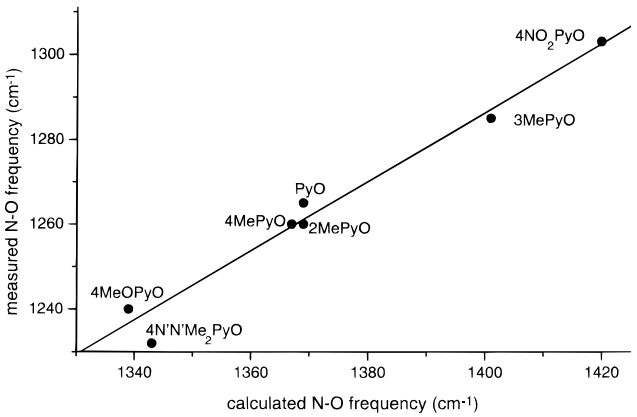

Figure 2. Correlation between calculated (with the 6-31G* basis set) and experimental N−O stretching frequency for the *N*-oxides studied. The solid line corresponds to the relation given by eq 9.

6-31+G*) does not result in significant geometry changes (Table 1). The 6-31G* geometric parameters of PyO are the same as calculated earlier by Lane et al.[24] in their ab initio study of pyridine, pyrazine, and their *N*-oxides.

The O···O distances of homoconjugated cations calculated with the 6-31G* basis set are about 0.1 Å greater than the experimental values. Inclusion of diffuse functions, which should stabilize charge separation that occurs when the homocomplex cation is formed (i.e., the use of the 6-31+G* basis set), does not change this (Table 1). Therefore the difference between the calculated and experimental values is probably caused by the absence of dynamic correlation, which we were unable to include in optimization, or by the compression of the homoconjugated cations in the crystal.

The N−O stretching frequencies of PyO and its derivatives calculated with the 6-31G* basis set are in good correlation with the experimental values[25,26] (Figure 2). The relationship between the calculated and experimental frequencies is given by eq 9. It should be noted that in the case of $4NMe_2PyO$, whose experimental N−O stretching frequency has the greatest deviation from the correlation line, the experimental frequency was determined with lesser accuracy.[26]

$$\nu_{obs} = 0.827(0.060)\nu_{calc} + 128(83)\ R = 0.987 \qquad (9)$$

where the numbers in parentheses are the standard deviations of the intercept and of the slope, respectively, and R is the correlation coefficient. Because the standard deviation of the intercept value is comparable with this value, the correlation indicates that the calculated frequencies should be scaled down by a factor of approximately 0.8 to achieve agreement between the calculated and experimental frequencies. For pyridine *N*-oxide the calculated N−O stretching frequency (1369 cm^{-1}) is overestimated by a similar amount with respect to the experimental value (1265 cm^{-1}; ref 25), as in the case of MP2 (1385 cm^{-1}) and Density Functional Theory (DFT) (1317 cm^{-1}) calculations of Szafran and Koput.[27] Thus, including correlation does not seem to improve the agreement between calculated and observed frequencies and the RHF method seems to give a fairly good description of the oscillations of the N−O bond.

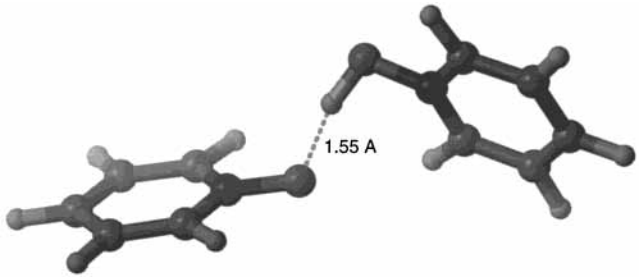

Figure 3. The equilibrium structure of the $PyOHPyO^+$ cation calculated with the 6-31G* basis set. The picture was prepared using MOLMOL.[38]

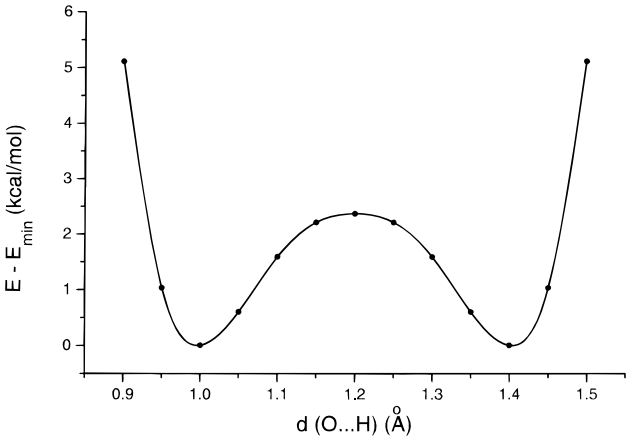

Figure 4. Energy variation on proton transfer in the O−H···O bridge of the pyridine *N*-oxide homoconjugated cation. Filled circles represent points where 6-31G* energies have been calculated.

Figure 3 shows the energy-optimized structure of the homoconjugated cation of pyridine *N*-oxide. As shown, despite the close approach of the two electronegative oxygen atoms, the hydrogen bond in the complex is not symmetric. The orientation angles of the two pyridine rings with respect to the O···O axis are not related by symmetry operations. Similar conclusions were drawn by Wasicki et al.[9] in their recent ab initio study of the homoconjugated cation of pyridine *N*-oxide. The calculated structures of the homoconjugated cations of the other derivatives of pyridine *N*-oxide are similar. The proton-transfer curve shown in Figure 4 indicates an energy barrier of 2.4 kcal/mol. After including the thermodynamic correction (eqs 7 and 8), the Gibbs free energy value at the maximum of the proton-transfer curve

TABLE 2: Calculated Protonation and Homoconjugation Energies and Gibbs Free Energies (kcal/mol) of Pyridine *N*-Oxide Derivatives (kcal/mol) and the pK_a and log K_h Values Determined in Acetonitrile (ref 1)

	ΔE_{prot}			ΔG_{prot}		ΔE_h			ΔG_h			
compound	RHF	MP2	SCRF	RHF	SCRF	RHF	MP2	SCRF	RHF	SCRF	pK_a	log K_h
PyO	−241.24	−226.76	−117.48	−232.94	−109.18	−33.99	−35.53	−12.36	−22.39	−0.76	10.04	3.22
PicO	−243.70	−228.60	−126.03	−235.40	−117.73	−32.91	−34.93	−6.92	−19.86	6.13	10.23	3.25
PicO	−243.61	−229.81	−122.66	−235.50	−114.55	−33.62	−34.65	−2.15	−21.37	10.10	10.31	3.35
PicO	−245.71	−230.96	−120.06	−237.31	−228.91	−34.17	−35.00	−5.60	−21.96	6.61	11.00	3.57
NO_2PyO	−223.38	−211.10	−113.70	−215.46	−105.78	−26.95	−27.27	[a]	−16.28	[a]	5.64	[b]
4MeOPyO	−250.38	−236.37	−120.06	−241.75	−111.43	−34.82	−36.36	−14.67	−23.72	−3.57	12.28	4.03
$4NMe_2PyO$	−260.10	−247.42	−128.38	−251.30	−119.58	−35.47	−37.77	[a]	−24.47	[a]	15.63	4.59

[a] Value could not be calculated because of convergence problems in SCF. [b] The equilibrium constant is indeterminably small.

becomes 1.2 kcal/mol lower compared with the values at minima. This suggests that the movement of the proton in the hydrogen-bonded bridge is unrestricted and that the hydrogen bond in the homoconjugated cation is effectively symmetric. These features agree with the fact that the O···H···O bridge is crystallographically symmetric[5,9] and with very broad O···H bands in the infrared spectra of *N*-oxide basic salts.[2,6,8,28,29]

The calculated energies and Gibbs free energies of proton transfer and homoconjugation, together with the values of the corresponding equilibrium constants measured in acetonitrile,[1] are summarized in Table 2. The values of these constants in acetonitrile were determined with the greatest accuracy, compared with other Parker solvents.[1] Moreover, the acid dissociation and cationic homoconjugation constants determined in various Parker solvents are linearly correlated[1,30,31] and it is therefore sufficient to compare the theoretically calculated Gibbs free energies with constants measured in one chosen solvent. The energies obtained from single-point MP2 calculations are also included in this table for comparison; as shown, including the dynamic correlation results in shifting the protonation and homoconjugation energies and not very much in changing energy relations. Because optimization was carried out at the RHF and not at the MP2 level, RHF energies are used in the later discussion.

As shown, the theoretically calculated values follow the variation of the equilibrium constants. The only exception is the placement of the homoconjugation Gibbs free energy of PyO, which is higher than that of the methyl derivatives and in disagreement with the order of experimentally measured homoconjugation-constant values in solution (Table 2). The corresponding correlation equations are as follows:

$$\mathrm{p}K_a = -0.273(0.016)\Delta G_{prot} - 53.7(3.9)\ R = -0.991 \quad (10)$$

$$\log K_h = -0.280(0.085)\Delta G_h - 2.6(1.9)\ R = -0.853 \quad (11)$$

It can therefore be concluded that the relatively inexpensive RHF ab initio calculations, without the inclusion of dynamic correlation or solvation effects, are sufficient to predict the variation of acid dissociation and homoconjugation constants in aprotic solvents. The correspondence between the calculated energies and the experimental pK_a and log K_h values does not improve after adding single-point MP2 correction (Table 2). It can also be noted that the energies and the Gibbs free energies of homoconjugation are linearly correlated with the energies and the Gibbs free energies, respectively, of protonation (i.e., the stronger the base the stronger homoconjugates it forms). The correlation equations are as follows:

$$\Delta E_h = 0.238(0.043)\Delta E_{prot} + 25(11)\ R = 0.926 \quad (12)$$

$$\Delta G_h = 0.235(0.042)\Delta G_{prot} + 34(9)\ R = 0.929 \quad (13)$$

Such correlations also hold between the pK_a and log K_h values determined in various nonaqueous solvents.[31]

The introduction of solvation in the SCRF spherical-cavity model does not improve the agreement between the variation of the calculated homoconjugation Gibbs free energies and that of the experimental log K_h values (Table 2). Moreover, some of the homoconjugation Gibbs free energies become positive, in contrast to the experimental log K_h values. We have also tried to use the more elaborate polarizable continuum model (PCM), in which the solute cavity is represented as a union of spheres;[32] however, the obtained solvation energies were even more inconsistent than in the case of the spherical-cavity model (e.g., the calculated solvation free energies of neutral compounds were sometimes more negative than the solvation free energies of their charged conjugated acids). Therefore, these results are not included in Table 2. This suggests that the mean-field electrostatic models are probably too crude to treat the case studied in this work. One reason for this could be the fact that the size of the solvent molecule (acetonitrile) is comparable with the size of the solute and the solvent cannot probably be treated as a continuous medium. Second, the differences between the protonation and homoconjugation energies in the series of compounds studied are relatively small and probably a more refined solvent model is required to reproduce them correctly. The drawbacks of continuum electrostatic solvation models were also reported by other authors.[33,34] A correct way to evaluate the solvation free energy could be Monte Carlo or molecular dynamics simulations with explicit solvent molecules and effective potential energy surface of intrasolute, solute−solvent, and solvent−solvent interaction derived from ab initio calculations. These studies are now being carried out in our laboratory.

Acknowledgment. This work was supported by grant no. PB 468/T09/96/10 from the Polish State Committee for Scientific Research (KBN). Calculations were carried out with the use of the resources and software at the Interdisciplinary Center for Molecular Modeling (ICM), Warsaw, Poland, the Informatics Center of the Metropolitan Academic Network (IC MAN) at the Technical University of Gdańsk.

References and Notes

(1) Chmurzyński, L. *Solvent Effect on Acidic−Basic Interactions of Substituted Pyridine N-Oxides*; University of Gdańsk: Gdańsk, Poland, 1994.
(2) Szafran, M.; Dega-Szafran, Z. *J. Mol. Struct.* **1983**, *99*, 189.
(3) Gilkerson W. R.; Ralph, E. K. *J. Am. Chem. Soc.* **1965**, *87*, 175.
(4) Pawlak, Z.; Wiśniewska, M.; Richert, M. *J. Chem. Thermodyn.* **1994**, *26*, 379.
(5) Jaskólski, M.; Gdaniec, M.; Kosturkiewicz, Z.; Szafran, M. *Pol. J. Chem.* **1978**, *53*, 2399.
(6) Speakman, J. C.; Muir, K. W. *Croat. Chem. Acta* **1982**, *55*, 233.
(7) Sakhawathussain, M.; Aziz al-Hamoud, S. A. *Inorg. Chim. Acta* **1984**, *82*, 111.
(8) Hussain, M. S.; Al-Hamoud, S. A. A. *J. Chem. Soc., Dalton Trans.* **1985**, 749.
(9) Wasicki J.; Jaskólski, M.; Pajak, Z.; Szafran, M.; Dega-Szafran, Z.; Adams, M. A.; Parker, S. F. *J. Mol. Struct.* **1999**, *476*, 81.
(10) Jaffé, H. H. *J. Am. Chem. Soc.* **1955**, *77*, 4445.
(11) Gardner, J. N.; Katritzky, A. R. *J. Chem. Soc.* **1957**, 4375.
(12) Chmurzyński, L.; Wawrzynów, A.; Pawlak, Z. *Electrochim. Acta* **1990**, *35*, 665.
(13) Liwo, A.; Sokołowski, K.; Wawrzynów, A.; Chmurzyński, L. *J. Solution Chem.* **1990**, *19*, 1113.
(14) Chmurzyński, L.; Liwo, A. *J. Chem. Soc., Faraday Trans. 2* **1991**, *87*, 1729.
(15) Chmurzyński, L.; Liwo, A.; Tempczyk, A. *Z. Naturforsch., B: Chem. Sci.* **1989**, *44b*, 1263.
(16) Chmurzyński, L.; Liwo, A. *Z. Naturforsch. B: Chem. Sci.* **1990**, *45b*, 717.
(17) Kaczmarczyk; E.; Wróbel, R.; Liwo, A.; Chmurzyński, L. *J. Mol. Struct.* **1999**, *477*, 113.
(18) Schmidt, M. W.; Baldridge, K. K.; Boatz, J. A.; Elbert, S. T.; Gordon, M. S.; Jensen, J. A.; Koseki, S.; Matsunaga, N.; Nguyen, K. A.; Su, S.; Windus, T. L.; Dupuis, M.; Montgomery, J. A. *J. Comput. Chem.* **1993**, *14*, 1347.
(19) Kirkwood, J. G. *J. Chem. Phys.* **1934**, *2*, 351.
(20) Onsager, L. *J. Am. Chem. Soc.* **1936**, *58*, 1486.
(21) Szafran, M.; Karelson, M. M.; Katritzky, A. R.; Koput, J.; Zerner, M. C. *J. Comput. Chem.* **1993**, *14*, 371.
(22) Karelson, M.; Tamm, T.; Zerner, M. C. *J. Phys. Chem.* **1993**, *97*, 11901.
(23) Reichardt, Ch. *Solvents and Solvent Effects in Organic Chemistry*; VCH Verlaggesellschaft GmbH: Weinheim, Germany, 1988; pp 407−410.
(24) Lane, P.; Murray, J. S.; Politzer, P. *J. Mol. Struct.: THEOCHEM* **1991**, 283.

(25) Ochiai, E. *Aromatic Amine Oxides*; Elsevier: Amsterdam, 1967; p 119.
(26) Katritzky, A. R.; Gardner, J. N. *J. Chem. Soc.* **1958**, 2192.
(27) Szafran, M.; Koput, J. *Pol. J. Chem.* **1998**, 368.
(28) Dega-Szafran, Z.; Hrynio, A.; Szafran, M. *Spectrochim. Acta A* **1987**, *43*, 1533.
(29) Dega-Szafran, Z.; Grundwald-Wyspiańska, M.; Szafran, M. *Bull. Pol. Acad. Sci. Chem.* **1994**, *42*, 269.
(30) Chmurzyński, L. *Anal. Chim. Acta* **1996**, *329*, 267.
(31) Chmurzyński, L. *Anal. Chim. Acta* **1996**, *334*, 155.
(32) Cammi, R.; Tomasi, J. *J. Comput. Chem.* **1995**, *16*, 1449.
(33) Yashuda, T.; Ikawa, S. *Chem. Phys.* **1998**, *238*, 173.
(34) Jhon, J. S.; Kang, Y. K. *J. Phys. Chem. A* **1999**, *103*, 5436.
(35) Chiang, J. F.; Song, J. J. *J. Mol. Struct.* **1982**, *96*, 151.
(36) Tsoucaris, G. *Acta Crystallogr.* **1961**, *14*, 914.
(37) Nakai, H.; Saito, T.; Yamakawa, M. *Acta Crystallogr., Sect. C (Cr. Str. Comm.)* **1988**, *44*, 533.
(38) Koradi, R.; Billeter, M.; Wüthrich, K. *J. Mol. Graphics* **1996**, *14*, 51.